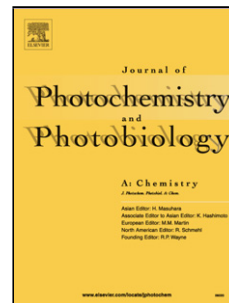


Accepted Manuscript

Title: 2-(2'-Hydroxyphenyl)-benzothiazole (HBT)-terpyridine conjugate: A highly specific ICT based fluorescent probe for Zn²⁺ ions and its application in confocal cell imaging

Authors: Sunanda Sahana, Gargi Mishra, Sri Sivakumar, Parimal K. Bharadwaj



PII: S1010-6030(17)31148-6
DOI: <https://doi.org/10.1016/j.jphotochem.2017.10.009>
Reference: JPC 10933

To appear in: *Journal of Photochemistry and Photobiology A: Chemistry*

Received date: 4-8-2017
Revised date: 6-10-2017
Accepted date: 7-10-2017

Please cite this article as: Sunanda Sahana, Gargi Mishra, Sri Sivakumar, Parimal K. Bharadwaj, 2-(2'-Hydroxyphenyl)-benzothiazole (HBT)-terpyridine conjugate: A highly specific ICT based fluorescent probe for Zn²⁺ ions and its application in confocal cell imaging, *Journal of Photochemistry and Photobiology A: Chemistry* <https://doi.org/10.1016/j.jphotochem.2017.10.009>

This is a PDF file of an unedited manuscript that has been accepted for publication. As a service to our customers we are providing this early version of the manuscript. The manuscript will undergo copyediting, typesetting, and review of the resulting proof before it is published in its final form. Please note that during the production process errors may be discovered which could affect the content, and all legal disclaimers that apply to the journal pertain.

2-(2'-Hydroxyphenyl)-benzothiazole (HBT)-terpyridine conjugate: A highly specific ICT based fluorescent probe for Zn²⁺ ions and its application in confocal cell imaging

Sunanda Sahana^a, Gargi Mishra^b, Sri Sivakumar^b and Parimal K. Bharadwaj^{a*}

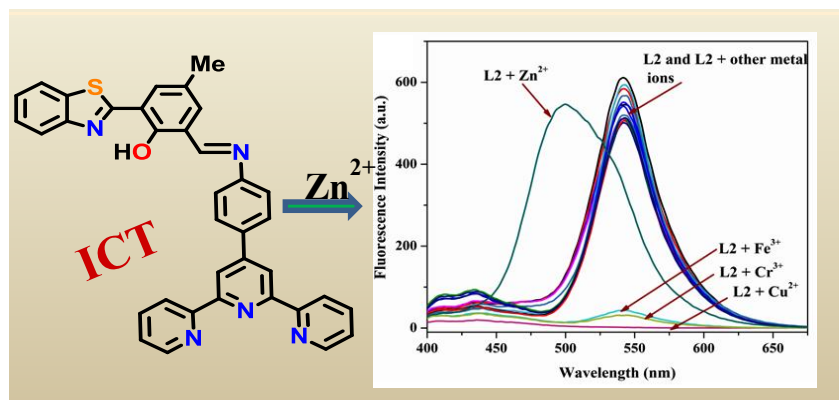
^aDepartment of Chemistry, Indian Institute of Technology Kanpur, Kanpur-208016, India

^bDepartment of Chemical Engineering, Indian Institute of Technology Kanpur, Kanpur-208016, India

* E-mail: pkb@iitk.ac.in

Graphical abstract

A benzothiazole-terpyridine conjugate is designed for Zn²⁺ ions sensor via internal charge transfer (ICT) mechanism with 42 nm blue-shift in emission spectra with a very low detection limit 35 nM within a biological pH range of 6-8.



Highlights

- One benzthiazole based chemosensor for Zn²⁺ probe has been synthesized.
- 1:1 stoichiometry of probe to Zn²⁺ was confirmed by ESI-MS.
- Exhibited a good binding constant and lowest detection limit towards Zn²⁺
- The probe is also able to function within a broad biological pH range of 6-8.

ABSTRACT

A new fluorescent sensor based on benzothiazole-terpyridine conjugate is reported. It functions as a fluorescent sensor that is highly selective for the Zn^{2+} ions *via* internal charge transfer (ICT) mechanism in DMSO: H_2O medium. The 42 nm blue-shifted emission upon addition of Zn^{2+} to the sensor is attributed to the capture of Zn^{2+} by the terpyridine moiety that inhibits ICT from the terpyridine to the benzthiazole moiety. The sensing is supported by the Job's plot, ESI-MS, 1H NMR titration experiments. Importantly, this probe shows high selectivity over other biologically relevant metal ions. Also, anions do not show any effect. In addition, the detection limit is found to be up to 35 nM which is acceptable within the EPA (US) limit. The probe is also able to function within a broad biological pH range of 6-8.

Keywords: Fluorescence; Internal Charge Transfer; Terpyridine; Zn^{2+} ions detection

1. Introduction

The zinc ions, as the second most abundant and essential trace element in the human body after iron, play a significant role in various fundamental biological processes, such as neurotransmission, cellular metabolism, enzyme regulation, gene expression and so on [1-233]. The disorder of Zn^{2+} metabolism leads to many neurological diseases, including Alzheimer's disease (AD), cerebral ischemia, and epilepsy [4-56]. There have been continuous efforts [7] to have better fluorescence chemosensors for the Zn^{2+} ions as direct and accurate spatiotemporal concentration of this metal ion can be made *via* fluorescence signaling in purposely built systems. [8-9101112].

Intramolecular charge-transfer (ICT) mechanism has been widely used as the basis for the design of ratiometric fluorescent sensors because metal binding to sensors induces a large shift in the absorption and fluorescence maxima [13-141516]. Ratiometric analysis reduces the environment-dependence, photo bleaching, variations in excitation intensity, emission collection

efficiency, and the physical or chemical fluctuations in the sample. Because of the intermolecular charge transfer (ICT) effect, ICT fluorophores with conjugated electron donor (D) and receptor (A) are able to display visible ICT absorption band and large Stokes shift in emission maxima. When a fluorophore contains an electron-donating group (donor) conjugated to an electron-withdrawing group (acceptor), it undergoes ICT from the donor to the acceptor upon excitation by light. The consequent change of the dipole moment leads to a larger Stokes shift, which is influenced by the microenvironment of the fluorophore. If the electron-rich terminal of the fluorophore interacts with a cation, a partial positive charge is photo-generated adjacent to the cation, and that affects the absorption or emission spectral wavelength of the fluorophore with an ICT excited state. So when a cation interacts with the donor group, the ground state is more stabilized than excited state, and this leads to blue shift of the absorption and emission spectra. Alternatively when a cation interacts with the electron withdrawing group (acceptor group), the excited state is more stabilized by the cation than in the ground state, and this leads to a red-shift of the absorption and emission spectra [17]. This mechanism is quite general, and therefore, the development of novel fluorescent sensors based on typical ICT fluorophore is an attractive and promising strategy [18-1920].

A series of novel heterocycle-based fluorescent dyes with donor- π -bridge-acceptor- (D- π -A) structural motif is reported, where benzothiazole serves as a strong electron-acceptor unit[21-2223].The strong electron withdrawing capability arises due to the unsymmetrical nature of the benzothiazole unit with nonzero dipolar moment and partially push-pull character. 2, 2': 6', 2'' - Terpyridine unit has gained much interest in recent years as typical metal-binding domain in the fields of supramolecular and coordination chemistry as well as materials science [24,25]. The

terpyridine unit possessing three near-coplanar nitrogen atoms, which has been widely used as building block for transition metal cations in supramolecular chemistry [26-27].

In this work, the ICT fluorophore, 2-(2'-Hydroxy-5'-methylphenyl) benzothiazole has been synthesized. To meet the demand of high selectivity toward Zn^{2+} , a strong chelator, i.e., 4-[2,2':6',2''-terpyridin]-4'-yl-benzenamine moiety has been incorporated into benzothiazole moiety to design D- π -A motif. When the terpyridine moiety coordinates to a Zn^{2+} , the electron density of that moiety will be decreased, lowering the electron-donating ability of the amine in the sensor leading to its detection.

2. Experimental

2.1. Materials and methods

Reagent grade, 2-hydroxy-5 methyl benzaldehyde and all metal perchlorate salts were acquired from Aldrich Chemicals (USA) and were used as received. 2-acetylpyridine, 4-nitrobenzaldehyde, 2-aminobenzenethiol, KOH, NH_4OH , $SnCl_2$, hexamine and the solvents were procured from S. D. Fine Chemicals (India). All the solvents were purified prior to use following standard procedures. The perchlorate metal salts are used in titration experiments. Chromatographic separations were done by column chromatography using silica gel (100-120 mesh) and basic alumina from S. D. Fine Chemicals (India). The variation of pH was achieved with dilute hydrochloric acid and sodium hydroxide. The reagents required for confocal cell imaging and MTT assay studies like Phosphate buffer saline, gelatin, Dulbecco's-modified eagle's medium (DMEM), penicillin-streptomycin antibiotic, 3-(4,5-dimethylthiazol-2-yl)-2,5 diphenyltetrazolium bromide (MTT) were also procured from Gibco.

All the synthesized compounds were characterized by various spectroscopic methods. Both ^1H NMR (500 MHz) and ^{13}C NMR spectra (125 MHz) of the compounds were recorded on a JEOL DELTA2 spectrometer in CDCl_3 with TMS as the internal standard. The ESI-MS data were obtained from a WATERS Q-Tof Premier Mass Spectrometer. UV-vis spectra were recorded on a Shimadzu 2450 UV-vis spectrophotometer at 21 °C. Fluorescence emission spectra were obtained on a Perkin-Elmer LS 50B Luminescence Spectrometer at 21 °C. The pH of different solutions were measured by using a pH meter model Eco testr pH I by Thermo Scientific (USA).

2.2. UV-vis and fluorescence spectroscopic studies

Luminescence properties of L2 were evaluated in DMSO: H_2O (3:2, v/v, 10 mM HEPES buffer, pH = 7)). Stock solution of L2 was prepared at a concentration of 10^{-3} M in 25 mL of DMSO and then diluted to the desired concentration. Stock solutions of various ions were prepared at the concentration of $\sim 10^{-4}$ M in 25 mL distilled water and then diluted to the desired concentrations. Absorbance and fluorescence spectral data were recorded 1 min after the addition of the ions. For fluorescence measurements, excitation wavelength was done at 360 nm (slit width = 10/10 nm) and emissions were acquired from 400 nm to 700 nm.

2.3. Synthesis

The probe L2 was synthesized in several steps as illustrated in Scheme 1.

2.3.1. Synthesis of 4'-(4-nitrophenyl)-2,2':6',2''-terpyridine (A)

The compound A was synthesized from a known procedure [28]. In a 500 mL round bottom flask, a mixture of 2-acetylpyridine (5 g, 41.5 mmol) and 4-nitrobenzaldehyde (3.17 g, 21 mmol) in CH_3OH (170 mL) was stirred vigorously with 15% aq. KOH (15 mL) and conc. NH_4OH (160 mL) for 3 days at room temperature. The deep brown colored precipitate was filtered and washed with

distilled water and then with cold methanol. The precipitate was further dissolved in 100 mL ethyl acetate. The organic fraction was washed with 1% NaHCO₃ solution three times. The organic layer was dried over anhydrous sodium sulphate. After complete removal of the solvent under vacuum, the crude brown product was recrystallized from absolute ethanol to give the pure product (Yield: 34%). m.p. 210–211 °C; ¹H NMR (500 MHz, CDCl₃) δ (ppm): 8.74 (m, 4H), 8.69 (d, J = 6.85 Hz, 2H), 8.37 (d, J = 8 Hz, 2H), 8.05 (d, J = 8 Hz, 2H), 7.90 (t, J = 7.4 Hz, 2H), 7.37 (t, J = 7.45, 2H) (Fig. S1). ¹³C NMR (125 MHz, CDCl₃, 25 °C, TMS) δ (ppm): 119.04, 121.51, 124.26, 128.39, 137.11, 145.58, 149.15, 155.78 (Fig. S2). ESI-MS: m/z (%): 355.1198 (100%) [M+H]⁺ (Fig. S3). Elemental analysis: calculated (%) for C₂₁H₁₄N₄O₂: C 71.16, H 3.98, N 15.82; found: C 71.55, H 3.76, N 15.75.

2.3.2. Synthesis of 4'-(4-aminophenyl)-2,2':6',2''-terpyridine (B)

In a 100 mL round bottom flask a mixture of compound A (0.46 g, 1.3 mmol) and SnCl₂ (1.536 g, 6.8 mmol) were taken in concentrated hydrochloric acid (12 mL) and then heated at 80° C for 8 h under nitrogen atmosphere. After cooling to room temperature, the reaction mixture was poured into cool water and adjusted to pH 8–9 by addition of NaHCO₃ solution. The reaction mixture was then extracted from 100 mL dichloromethane (three times). The organic layer was dried over anhydrous sodium sulphate. After complete removal of solvent a brown solid was obtained which was purified by column chromatography (basic alumina, eluting with hexane /ethyl acetate = 1:1) to give the pure product (Yield: 62%). m.p. 253–254 °C; ¹H NMR (500 MHz, CDCl₃) δ (ppm): 8.72 (d, J = 4 Hz, 2H), 8.67 (s, 2H), 8.66 (d, J = 8 Hz, 2H), 7.86 (t, J = 8 Hz, 2H), 7.78 (d, J = 8.55 Hz, 2H), 7.33 (t, J = 6.85 Hz, 2H), 6.80 (d, J = 8.6 Hz, 2H) (Fig. S4). ¹³C NMR (125 MHz, CDCl₃, 25 °C, TMS) δ (ppm): 115.32, 117.88, 121.44, 123.75, 128.47, 136.90, 149.15, 155.72 (Fig. S5).

ESI-MS: m/z (%): 325.1440 (100%) $[M+H]^+$ (Fig. S6). Elemental analysis: calculated (%) for $C_{21}H_{16}N_4$: C 77.81, H 4.97, N 17.28; found: C 77.88, H 4.93, N 17.32.

2.3.3. Synthesis of 2-(2'-benzothiazolyl)-4-methyl- phenol (C)

To a 30 mL ethanolic solution of 2-aminobenzenethiol (109 mg, 1.00 mmol), 2-hydroxy-5-methylbenzaldehyde (136 mg, 1.00 mmol) was added at room temperature under nitrogen atmosphere. The mixture was allowed to stir for 30 min at RT and then treated with hydrogen peroxide (30%) (2.31 mL, 74.8 mmol) and hydrochloric acid (37.5%) (1.14 mL, 37.3 mmol). The reaction mixture was stirred for 3h to obtain a yellow-green precipitate. The reaction mixture was then poured into crushed ice and then extracted three times with ethyl acetate (EtOAc). The organic layer was dried over anhydrous sodium sulphate and the crude product was purified by column chromatography (silica gel, 100 -200 mesh, EtOAc: hexane = 4:96, v/v) as a pale-yellow crystalline solid. (yield :51 %). Mp 127-128 °C. 1H NMR (500 MHz, $CDCl_3$) δ (ppm): 10.60 (s, 1H), 8.07 (d, $J = 7.85$ Hz, 1H), 7.99 (d, $J = 8.0$ Hz, 1H), 7.60 (t, $J = 8.62$ Hz, 1H), 7.52 (t, $J = 5.65$ Hz, 1H), 7.39 (s, 1H), 7.06 (d, $J = 9.0$ Hz, 1H), 6.87 (d, $J = 8.3$ Hz, 1H), 2.36 (s, 3H) (Fig. S7). ^{13}C NMR (125 MHz, $CDCl_3$, 25 °C, TMS) δ (ppm): 20.53, 117.80, 121.59, 122.13, 125.58, 126.80, 128.40, 133.94, 150.40, 158.40, 165.58 (Fig. S8). ESI-MS: m/z (%): 242.0647 (100%) $[M+H]^+$ (Fig. S9). Elemental analysis: calculated (%) for $C_{14}H_{11}NOS$: C 69.75, H 4.59, N 5.81; found: C 69.78, H 4.53, N 5.72

2.3.4. Synthesis of 3-(2-benzothiazolyl)-2-hydroxy-5-methyl- benzaldehyde (D)

In a 250 mL round bottom flask, compound C (0.5 g, 2.19 mmol) was dissolved in 50 mL trifluoroacetic acid and then hexamine (1.8 g, 12.85 mmol) was added in portion wise. The resulting solution was refluxed for 36 h at 145 °C under N_2 atmosphere till it turned dark brown. The reaction mixture was then allowed to cool to RT and poured into 100 ml 4 (N) HCl solutions.

The reaction mixture was extracted with ethyl acetate (EtOAc). The organic layer was dried over anhydrous sodium sulphate and the crude product was purified by column chromatography (hexane:ethyl acetate 5:1, v/v) to afford the pure product as a yellow solid (yield: 67%). m.p 176–178 °C. ¹H NMR (500 MHz, CDCl₃) δ (ppm): 12.95 (s, 1H), 10.69 (s, 1H), 8.80 (s, 1H), 7.98 (d, J = 10.5 Hz, 1H), 7.91 (d, J = 9.55 Hz, 1H), 7.63 (s, 1H), 7.52 (t, J = 9.05 Hz, 1H), 7.43 (t, J = 9.52 Hz, 1H), 2.61 (s, 3H) (Fig. S10). ¹³C NMR (125 MHz, CDCl₃, 25 °C, TMS) δ (ppm): 20.33, 117.80, 121.59, 122.13, 125.58, 126.80, 133.13, 150.59, 158.40, 166.80 (Fig. S11). ESI-MS: m/z (%): 270.0588 (100%) [M+H]⁺(Fig. S12). Elemental analysis: calculated (%) for C₁₅H₁₁NO₂S: C 66.89, H 4.12, N 5.03; found: C 66.83, H 4.13, N 5.02.

2.3.5. Synthesis of L2

In 100 mL round bottom flask compound D (0.5 g, 1.85 mmol) was dissolved in a mixed solvent containing 25mL absolute ethanol and 5 mL dry chloroform. Then compound B (0.66 g, 2.03 mmol) was added and the reaction mixture was refluxed for 48 h under nitrogen atmosphere. A deep orange colored precipitate was obtained. The precipitate was filtered off and washed with ice-cold absolute ethanol. The product was recrystallized from ethanol (Yield: 74%). m.p. 230–231 °C.

¹H NMR (500 MHz, CDCl₃) δ (ppm):10.78 (s, 1H), 8.82 (s, 2H), 8.78(s, 1H), 8.75 (d, J= 6.5 Hz, 2H), 8.70 (d, J = 8.0 Hz, 2H), 8.11 (d, J = 8.0 Hz, 1H), 8.03 (d, J = 8.8 Hz, 1H), 7.98 (d, J = 8.0 Hz, 2H), 7.91 (d, J=6.6 Hz, 2H), 7.89 (t, J= 6.82 Hz, 2H), 7.52 (t, J= 7.11 Hz, 1H), 7.45 (s, 1H) 7.41(t, J= 6.45 Hz, 1H), 7.37 (t, J= 6.70 Hz, 2H), 7.29 (s, 1H) 2.34 (s, 3H) (Fig.S13).

¹³C NMR (125 MHz, CDCl₃, 25 °C, TMS) δ (ppm):29.77,105.11,110.08,118.69,121.49,121.54,121.85,123.99,128.61,134.94,137,141.54,145.69,149.24,153.99,157.72, 168.61 (Fig. S14). ESI-

MS: m/z (%): 576.1874 (100%) [M+H]⁺(Fig. S15). Elemental analysis: calculated (%) for C₃₆H₂₅N₅OS: C 75.11, H 4.38, N 12.17; found: C 75.20, H 4.33, N 12.13.

2.4 Cell imaging

For potential application of the probe L2 in biological samples, the intracellular confocal imaging studies of L2 have been carried out in the presence of Zn²⁺. For this purpose, HeLa cells were cultured in DMEM medium containing penicillin/streptomycin (1% v/v) and FBS (10% v/v) in 5% CO₂ at 37 °C. About 10⁴ cells were seeded in each well of the 24 well tissue culture plates and incubated for 6 h in a CO₂ incubator. After 6 h, HeLa cells were incubated with zinc perchlorate salt (10 μM) dispersed in HEPES buffer (10 mM) which was added to the cell culture media. After 18 h, the media was removed from the plate and fresh media with L2 (10 μM) was added and incubated for 1 h. After 1 h, cells were washed with PBS, and fixed with 4 % formaldehyde solution for 20 min. The cells were imaged with confocal microscope Zeiss LSM 710. The images of the cell were recorded upon excitation at 360 nm. For green emission 488 nm argon laser was used and for red emission 543 helium neon laser was used.

2.5 MTT assay for cell viability assessment

For cytotoxicity assessment of biosensor L2, the HeLa cells (cervical cancer cell line) are chosen which have been used for testing toxicity of biosensors under vitro conditions [29,30]. Different concentrations of the sensor, ranging from (0-100 μM) of stock solutions were added to the cultured HeLa cells. A set of untreated control cells were also kept which were devoid of any exposure to any concentration of the sensors. 10⁴ cells were seeded in each well of 96 well plates and exposed to different concentrations of sensors (0- 100 μM) for 24 h. After 24 h, MTT (0.5 μg/ml) dispersed in plain DMEM media was added into each well and plate was incubated at 37 °C for 4 h. After 4 h, media containing dye was removed and 100 μl of DMSO was added to each

well and incubated for 20 min to dissolve the formazon crystals. The purple complex formed was read spectrophotometrically by taking absorbance of each at 376 nm using ELISA reader (Thermo scientific, Multiskan ELISA, USA). The percentage of cell viability was calculated as: (mean experimental absorbance/mean control absorbance) \times 100%. No significant difference was observed between the percentages of viable cells in the sensor-treated and control samples indicating thereby that the chemosensor L2 is non-cytotoxic and suitable for biological use.

3. Result and discussion

3.1. Photophysical properties

The photophysical properties of compound L2 were measured using UV-vis and fluorescence spectroscopy in DMSO: H₂O (3:2, v/v, 10 mM HEPES buffer, pH = 7) medium. The binding, recognition, and selectivity of L2 toward metal ions, including Cd²⁺, Zn²⁺, Na⁺, K⁺, Ca²⁺, Mg²⁺, Mn²⁺, Fe²⁺, Hg²⁺, Pb²⁺, Ag⁺, Al³⁺, Fe³⁺, Ni²⁺, Cu²⁺, Co²⁺, and Cr³⁺ were investigated. The absorption spectra of benzthiazole-terpyridine dye in presence of different metal ions are shown in Fig. 1a. In general the dye L2 displays an intense absorption spectrum at 467 nm corresponds to intramolecular-charge transfer (ICT) from the terpyridine moiety to the electron-withdrawing benzothiazole group. Upon addition of Zn²⁺ the color of the solution changes from colourless to yellow and discernible 91 nm blue shift of absorption peak is observed. This hypsochromic shift can be primarily ascribed due to the attachment of terpyridine moiety of dye molecule with Zn²⁺ *via* three near-coplanar nitrogen atoms. A similar but less pronounced blue shift (34 nm) is also observed in presence of Cd²⁺ ions. The other metal ions do not show significant shift.

The emission spectrum of free L2 exhibits a band with maxima positioned around 542 nm upon excitation at 360 nm. The examined alkali, alkaline earth and most transition metal ions show no

changes relative to L2, whereas the emission intensity of L2 is completely quenched by Cu^{2+} , Cr^{3+} , and Fe^{3+} ions. Interestingly, Zn^{2+} shows a 42 nm blue-shift of the band due to intramolecular charge transfer (ICT) from the Zn^{2+} coordinated terpyridine core to electron-withdrawing benzthiazole moiety at higher energy region. Therefore, L2 behaves as a ratiometric fluorescent sensor for the Zn^{2+} ions

To utilize L2 as an effective ion-selective fluorescence chemosensor for Zn^{2+} , the effect of competing metal ions was investigated. For this purpose, L2 was treated with Zn^{2+} in the presence of other various biologically and environmentally relevant metal ions in excess concentration in a mixed DMSO/water solution. Relatively low interference is observed for the detection of Zn^{2+} in the presence of other metal ions (Fig. 2a). Thus L2 can be used as a selective fluorescent sensor for Zn^{2+} in the presence of most competing metal ions. The possible interference of anions was also probed by the competitive experiments which clearly demonstrate that the emission profile of L2- Zn^{2+} solution remains unchanged by the presence of common anions such as NO_3^- , NO_2^- , SO_3^{2-} , SO_4^{2-} , CO_3^{2-} , HCO_3^- , F^- , Cl^- , Br^- , I^- , OAc^- , PO_4^{3-} , and CrO_4^{2-} (Fig.2b).

The titration of Zn^{2+} with L2 (2 μM) shows a strong fluorescence enhancement with the increase of the Zn^{2+} concentration range (0-50 μM). The fluorescence titration curve reveals that the fluorescence intensity at 542 nm is totally diminished and at 500 nm, increased linearly with increasing concentration of Zn^{2+} ions (Fig.3b). In the case of absorption titration, where the absorption peak at 376 nm is gradually intensified with increasing concentration range (5-50 μM) (Fig.3a).

The method of continuous variation (Job's plot) was also done to prove the 1:1 stoichiometry (Fig. 4). The binding mode of Zn^{2+} ions with receptor L2 is also proved by mass spectroscopy (Fig.S16). The mass spectrum shows an intense peak at m/z 739.33 corresponding to the $[L2 + Zn^{2+} + OClO_3^-]^+$ complex which not only confirms the binding of Zn^{2+} ions with receptor L2 but also proved the 1:1 stoichiometry of host and guest species.

The association constant for Zn^{2+} was estimated to be $9.95 \times 10^5 M^{-1}$ on the basis of linear fitting of the fluorescence titration (Fig. 5a) curve using Benesi–Hildebrand plot and demonstrated that 1:1 stoichiometry (host/guest) is the most stable species in the solution [31]. To evaluate the sensing properties of L2 for Zn^{2+} , the limit of detection (LOD) of L2 for Zn^{2+} was also measured. The detection limit of the probe for Zn^{2+} was evaluated from the fluorescence titration and calculated to be 35 nM (Fig.5b) using the equation $DL = K \times Sb1/S$, where $K = 3$, and $Sb1$ is the standard deviation of 10 replicate blank solution and S is the slope of the calibration curve in the lower region.

The direct evidence to determine the mode of complexation, 1H NMR titrations of L2 with various concentrations of Zn^{2+} was also studied in $CDCl_3$. As shown in Fig. 6, the characteristic peaks of terpyridine protons at 8.76, 8.72, 8.66, 7.47 ppm shifted to a lower field after the coordination of L2 with Zn^{2+} ions. Similar shifts upon metal binding are observed in other cases [32]. However the proton signal at 10.6954 ppm due $-OH$ group in benzthiazole moiety was almost unaltered suggesting phenolate O atom not bound to Zn^{2+} ions. These observed downfield shifts of various protons suggest 1:1 binding stoichiometry for L2: Zn^{2+} and tri-coordination of Zn^{2+} to L2 through three near-coplanar nitrogens of terpyridine unit. The tetra-coordination of Zn^{2+} is satisfied by perchlorate counter anion.

3.3. Reversibility

In order to obtain a better understanding of the interactions between L2 and Zn^{2+} , we have studied the chemical reversibility of the binding of L2 to Zn^{2+} in DMSO: H_2O (3:2, v/v, 10 mM HEPES buffer, pH = 7) (Fig. 7). As seen by the naked eye, the yellow color of a solution of L2- Zn^{2+} gradually disappeared followed by red shift of emission spectra upon the addition of excess disodium EDTA (10 equivalents).

3.4. Density functional theory

In parallel to the experimental study, to further understand the electronic structures of L2 and L2- Zn^{2+} complex DFT calculation were performed using the Gaussian 09 programme [33]. The L2 was optimized with the B3LYP [34-3536373839] functional and 6-311+G (d,p) basis set. For Zn^{2+} bound species with L2, LANL2DZ for Zn^{2+} and 6-31g*+ for the rest of the atoms were used for optimization. The optimized structure of L2 with Zn^{2+} is shown in Fig. 8. The bond lengths of Zn-N bonds are similar to the reported complex [40].

3.5. Effect of pH

In addition to metal ion selectivity, the pH-insensitivity of fluorescence in near neutral and weak acidic media is of importance for practical applications both in environmental and biological analysis. Thus we have measured the fluorescence intensity of L2 at various pH values in the presence and absence of Zn^{2+} . The fluorescence intensity of the L2 at 542 nm decreases under acidic condition due to protonation of nitrogen atoms of terpyridine moiety. In the neutral to alkaline medium it shows moderate fluorescence intensity at 542 nm (Fig. 9a). Interestingly, L2 shows good fluorescence sensing ability to Zn^{2+} at 500 nm over a wide range of pH values from 6 to 9. As shown in Fig. 9b, L2 shows little sensing ability to Zn^{2+} at a pH below 6.0, which may be

due to protonation, but exhibits satisfactory Zn^{2+} sensing abilities when the pH is increased to the range 6 -8.

3.6. Confocal Imaging Studies

The Zn^{2+} detection capability of probe L2 in living cells was evaluated by confocal microscopy. HeLa cells incubated with L2 (10 μ M) exhibits bright fluorescence in red channel upon excitation at 360 nm but very weak fluorescence in green channel. However a bright fluorescence signal is observed in green channel when the cells strained with L2 and Zn^{2+} (10 μ M) , which suggests that probe is cell membrane permeable and can be efficiently applied in imaging of Zn^{2+} in living cells (Fig. 10). The cells incubated with both L2 and Zn^{2+} show considerable weak fluorescence in red channel. Hence, this approach of bio sensing using L2 of Zn^{2+} ions can potentially be used for *in vitro* and *in vivo* diagnostics of accumulation of Zn^{2+} ions.

Additionally, MTT assessment for finding the toxicity of the biosensor was carried out to check if sensor itself induces any cytotoxicity in cells. It was observed that the proliferation of HeLa cells is not affected by the addition of this sensor in the *in vitro* cell culture conditions in the relevant working concentrations (5-20 μ M). Thus the sensor induces negligible toxicity in HeLa cells and the cell proliferation is almost ~ 90 % of the negative control (samples which did not contain any biosensors) (Fig.11). From this result it can be concluded that sensor is not cytotoxic and also able to perform fluorescence based detection of Zn^{2+} ions in *in vitro* conditions.

4. Conclusion

In summary, we have presented a fluorescent sensor with terpyridine substituent groups as a fluorescent ratiometric sensor for detection of Zn^{2+} based on an internal charge transfer (ICT) mechanism in DMSO: H₂O medium. The 42 nm blue-shift emission upon addition of Zn^{2+} to L2 is attributed to the capture of Zn^{2+} by a terpyridine moiety leading to diminished electron donating

ability. The Zn^{2+} ion sensing mechanism is also supported by the Job' plot, ESI-MS, 1H NMR titration experiments. Importantly, this probe shows high selectivity over other anions; moreover, this selectivity is retained even in the presence of other biologically relevant metal ions. A comparison study for recent ICT based chemosensors for Zn^{2+} is also shown (Table 1 in SI). In addition the detection limit of L2 was found to be upto 35 nM which is acceptable within the USEPA limit. The probe is also able to work in a broad biological pH range of 6-8.

Acknowledgements

This work was supported by Department of Science and Technology, New Delhi, India (No. SERB/CHM/20130239 to P. K. B). S.S. thanks Council of Scientific and Industrial Research (CSIR) India for senior research fellowship. For Gaussian calculation HPC 2010 facility of IIT Kanpur is gratefully acknowledged.

References

- [1] J. M. Berg, Y. Shi, The Galvanization of Biology: A Growing Appreciation for the Roles of Zinc, *Science*. 271 (1996) 1081-1085.
- [2] B. L. Vallee, K. H. Falchuk, The biochemical basis of zinc physiology, *Physiol. Rev.* 73 (1993) 79-118.
- [3] W. Maret, Zinc coordination sphere in biochemical zinc sites, *Biometals*. 14 (2001) 187-190.
- [4] A. I. Bush, W. H. Pettingell, G. Multhaup, M. D. Paradis, J. P. Vonsattel, J. F. Gusella, K. Beyreuther, C. L. Masters, R. E. Tanzi, Rapid induction of Alzheimer A beta amyloid formation by zinc, *Science*. 265 (1994) 1464-1467.
- [5] R. A. Cherny, J. T. Legg, C. A. McLean, D. P. Fairlie, X. Huang, C. S. Atwood, K. Beyreuther, R. E. Tanzi, C. L. Masters, A. I. Bush, Aqueous Dissolution of Alzheimer's Disease Ab Amyloid Deposits by Biometal Depletion, *J. Biol. Chem.* 274 (1999) 23223-23228.
- [6] V. Tõugu, A. Karafin, P. Palumaa, Binding of zinc(II) and copper(II) to the full-length Alzheimer's amyloid- β peptide, *J. Neurochem.* 104 (2008) 1249-1259.
- [7] Z. Xu, J. Yoon, D. R. Spring, Fluorescent chemosensors for Zn^{2+} , *Chem. Soc. Rev.* 39 (2010) 1996-2006.

- [8] X. Tian, Q. Zhang, M. Zhang, K. Uvdal, Q. Wang, J. Chen, W. Du, B. Huang, J. Wu, Y. Tian, Probe for simultaneous membrane and nucleus labeling in living cells and in vivo bioimaging using a two-photon absorption water-soluble Zn(II) terpyridine complex with a reduced π -conjugation system, *Chem. Sci.* 8 (2017) 142–149.
- [9] C. Patra, A. K. Bhanja, A. Mahapatra, S. Mishra, K. Das Saha, C. Sinha, Coumarinyl thioether Schiff base as a turn-on fluorescent Zn(II) sensor and the complex as chemosensor for the selective recognition of ATP, along with its application in whole cell imaging, *RSC Adv.* 6 (2016) 76505–76513.
- [10] G. Ambrosi, M. Formica, V. Fusi, L. Giorgi, E. Macedi, M. Micheloni, P. Paoli, P. Rossi, A Biphenol-Based Chemosensor for Zn^{II} and Cd^{II} Metal Ions: Synthesis, Potentiometric Studies, and Crystal Structures, *Inorg. Chem.* 55 (2016) 7676–7687.
- [11] A. Jana, B. Das, S. K. Mandal, S. Mabhui, A. R. Khuda-Bukhsh, S. Dey, Deciphering the CHEF-PET-ESIPT liaison mechanism in a Zn²⁺ chemosensor and its applications in cell imaging study, *New J. Chem.* 40 (2016) 5976–5984.
- [12] R. Balamurugan, W. Chang, Y. Zhang, S. Fitriyani and J. Liu, A turn-on fluorescence chemosensor based on a tripodal amine [tris(pyrrolyl- α -methyl)amine]- rhodamine conjugate for the selective detection of zinc ions, *Analyst.* 141 (2016) 5456–5462.
- [13] H. H. Wang, L. Xue, Y. Y. Qian, H. Jiang, Novel Ratiometric Fluorescent Sensor for Silver Ions, *Org. Lett.* 12 (2010) 292-295.
- [14] C. Lu, Z. Xu, J. Cui, R. Zhang and X. Qian, Ratiometric and Highly Selective Fluorescent Sensor for Cadmium under Physiological pH Range: A New Strategy to Discriminate Cadmium from Zinc, *J. Org. Chem.* 72 (2007) 3554-3557.
- [15] J. Wang, H. Liu, W. Wang, I. Kim, C. Ha, A thiazoline-containing cobalt(II) complex based colorimetric fluorescent probe: “turn-on” detection of fluoride, *Dalton Trans.* (2009) 10422-10425.
- [16] S. Goswami, D. Sen, N. K. Das, A New Highly Selective, Ratiometric and Colorimetric Fluorescence Sensor for Cu²⁺ with a Remarkable Red Shift in Absorption and Emission Spectra Based on Internal Charge Transfer, *Org. Lett.* 12 (2010) 856-859.
- [17] B. Valeur, I. Leray, Design principles of fluorescent molecular sensors for cation recognition, *Coord. Chem. Rev.* 205 (2000) 3-40.
- [18] K. Komatsu, Y. Urano, H. Kojima, T. Nagano, Development of an Iminocoumarin-Based Zinc Sensor Suitable for Ratiometric Fluorescence Imaging of Neuronal Zinc, *J. Am. Chem. Soc.* 129 (2007) 13447-13454
- [19] G. Zhang, H. Li, S. Bi, L. Song, Y. Lu, L. Zhang, J. Yua, L. Wang, A new turn-on fluorescent chemosensor based on diketopyrrolopyrrole (DPP) for imaging Zn²⁺ in living cells, *Analyst.* 138 (2013) 6163–6170.
- [20] D. Maity, T. Govindaraju, Pyrrolidine constrained bipyridyl-dansyl click fluoroionophore

- [21] P. Zhou, Z. Zhang, Y. Li, X. Chen, J. Qin, Thiophene-Fused Benzothiadiazole: A Strong Electron-Acceptor Unit to Build D–A Copolymer for Highly Efficient Polymer Solar Cells, *Chem. Mater.* 26 (2014) 3495–3501.
- [22] P. Ledwon, P. Zassowski, T. Jarosz, M. Lapkowski, P. Wagner, V. Cherpak, P. Stakhira, A novel donor–acceptor carbazole and benzothiadiazole material for deep red and infrared emitting applications, *J. Mater. Chem. C.* 4 (2016) 2219–2227.
- [23] P. Sonar, E. L. Williams, S. P. Singh, A. Dodabalapur, Thiophene–benzothiadiazole–thiophene (D–A–D) based polymers: effect of donor/acceptor moieties adjacent to D–A–D segment on photophysical and photovoltaic properties, *J. Mater. Chem.* 21 (2011) 10532–10541.
- [24] S. M. Brombosz, A. J. Zuccherro, R. L. Phillips, D. Vazquez, A. Wilson, U. H. F. Bunz, Terpyridine-Based Cruciform–Zn²⁺ Complexes as Anion-Responsive Fluorophores, *Org. Lett.* 9 (2007) 4519–4522.
- [25] T. D. Rao, L. J. Liang, L. Y. Zhang, Ratiometric fluorescence recognition for pyrophosphate on the basis of terpyridine derivative, *Anal. Sci.* 29 (2013) 1165–1169.
- [26] H. Hofmeier, U. S. Schubert, Recent developments in the supramolecular chemistry of terpyridine–metal complexes, *Chem. Soc. Rev.* 33 (2004) 373–399.
- [27] J. L. Liang, X. J. Zhao, C. Z. Huang, Zn(II) complex of terpyridine for the highly selective fluorescent recognition of pyrophosphate, *Analyst.* 137 (2012) 953–958.
- [28] X. -C. Zhang, Z. -M. Huo, T. -T. Wang, H. -P. Zeng, Facile synthesis and photochromic properties of diarylethene-containing terpyridine and its transition metal (Zn²⁺ /Co²⁺/Ru²⁺) complexes, *J. Phys. Org. Chem.* 25 (2012) 754–759.
- [29] S. Anbu, R. Ravishankaran, M. F. C. Guedes da Silva, A. A. Karande, A. J. L. Pombeiro, Differentially Selective Chemosensor with Fluorescence Off–On Responses on Cu²⁺ and Zn²⁺ Ions in Aqueous Media and Applications in Pyrophosphate Sensing, Live Cell Imaging, and Cytotoxicity, *Inorg. Chem.* 53 (2014) 6655–6664.
- [30] S. Anbu, S. Shanmugaraju, R. Ravishankaran, A. A. Karande, P. S. Mukherjee, Naphthylhydrazone based selective and sensitive chemosensors for Cu²⁺ and their application in bioimaging, *Dalton Trans.* 41 (2012) 13330–13337.
- [31] H. A. Benesi, J. H. Hildebrand, A Spectrophotometric Investigation of the Interaction of Iodine with Aromatic Hydrocarbons, *J. Am. Chem. Soc.* 71 (1949) 2703–2707.
- [32] S. Yin, J. Zhang, H. Feng, Z. Zhao, L. Xu, H. Qiu, B. Tang, Zn²⁺-selective fluorescent turn-on chemosensor based on terpyridine-substituted siloles, *Dyes. Pigm.* 95 (2012) 174–179.
- [33] M. J. Frisch, G. W. Trucks, H. B. Schlegel, G. E. Scuseria, M. A. Robb, J. R. Cheeseman, G. Scalmani, V. Barone, B. Mennucci, G. A. Petersson, H. Nakatsuji, M. Caricato, X. Li, H. P. Hratchian, A. F. Izmaylov, J. Bloino, G. Zheng, J. L. Sonnenberg, M. Hada, M. Ehara, K. Toyota, R. Fukuda, J. Hasegawa, M. Ishida, T. Nakajima, Y. Honda, O. Kitao, H. Nakai, T. Vreven, J. A. Montgomery, Jr., J. E. Peralta, F. Ogliaro, M. Bearpark, J. J. Heyd, E. Brothers, K.

N. Kudin, V. N. Staroverov, T. Keith, R. Kobayashi, J. Normand, K. Raghavachari, A. Rendell, J. C. Burant, S. S. Iyengar, J. Tomasi, M. Cossi, N. Rega, J. M. Millam, M. Klene, J. E. Knox, J. B. Cross, V. Bakken, C. Adamo, J. Jaramillo, R. Gomperts, R. E. Stratmann, O. Yazyev, A. J. Austin, R. Cammi, C. Pomelli, J. W. Ochterski, R. L. Martin, K. Morokuma, V. G. Zakrzewski, G. A. Voth, P. Salvador, J. J. Dannenberg, S. Dapprich, A. D. Daniels, O. Farkas, J. B. Foresman, J. V. Ortiz, J. Cioslowski and D. J. Fox, Gaussian 09, Revision D.01, Gaussian, Inc., Wallingford, CT, 2013.

[34] A. D. Becke, Density-functional thermochemistry. III. The role of exact exchange, *J. Chem. Phys.* 98 (1993) 5648-5652.

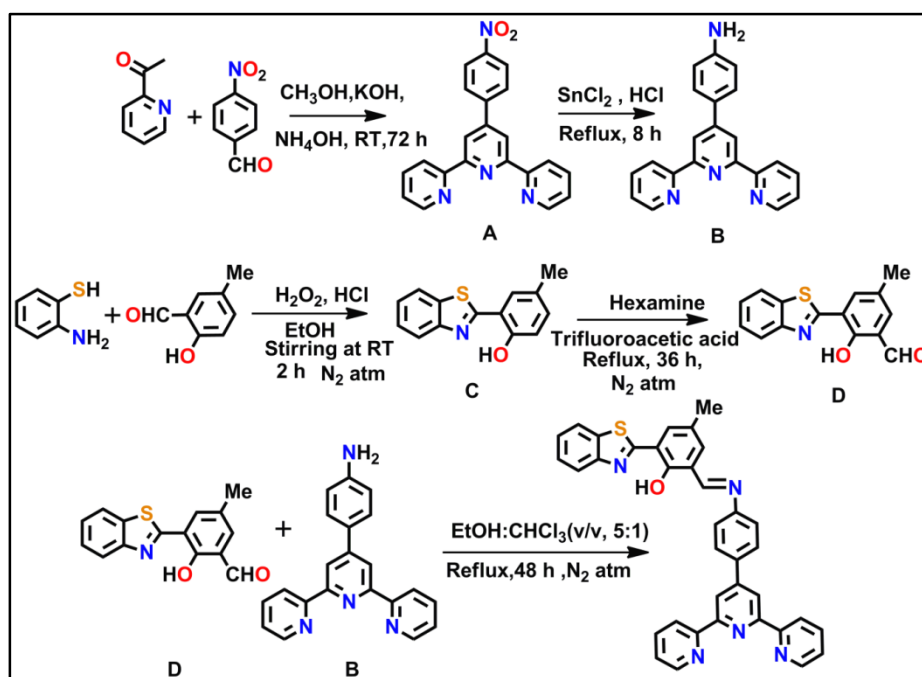
[35] C. Lee, W. Yang, R. G. Parr, Development of the Colle-Salvetti correlation-energy formula into a functional of the electron density, *Phys. Rev. B. Condens. Matter.* 37 (1988) 785-789.

[36] D. Andrae, U. Haeussermann, M. Dolg, H. Stoll, H. Energy-adjusted ab initio pseudopotentials for the second and third row transition elements, *Preuss, Theor. Chim. Acta.* 77 (1990) 123-141.

[37] M. Cossi, N. Rega, G. Scalmani, V. Barone, Energies structures, and electronic properties of molecules in solution with the C-PCM solvation model, *J. Comput. Chem.* 24 (2003) 669-681.

[38] M. Cossi, V. Barone, Time-dependent density functional theory for molecules in liquid solutions, *J. Chem. Phys.* 115 (2001) 4708-4717.

[39] V. Barone, M. Cossi, Quantum calculation of molecular energies and energy gradients in solution by a conductor solvent model, *J. Phys. Chem. A.* 102 (1998) 1995-2001.



Scheme 1. Synthetic scheme of the probe L2

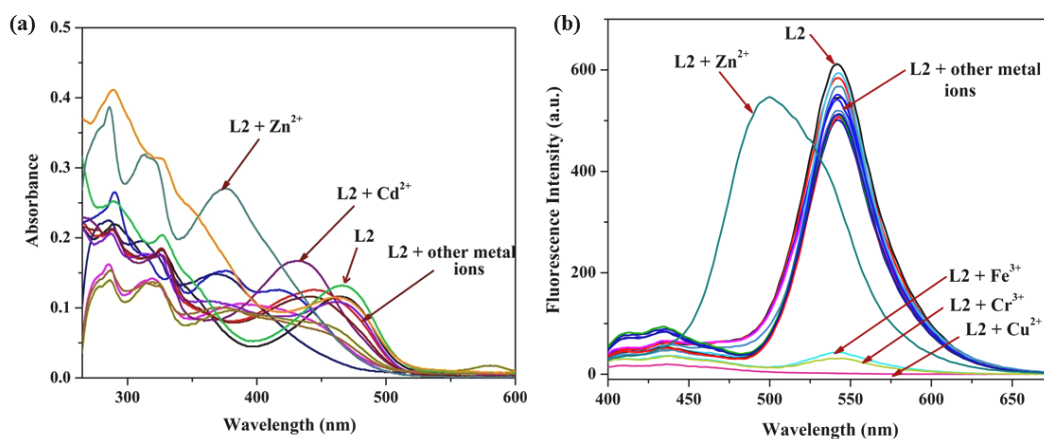


Fig. 1. (a) Absorption spectra of L2 (10 μM) in DMSO: H₂O (3:2, v/v, 10 mM HEPES buffer, pH = 7) in the presence of 3 equivalents of various metal ions. (b) Fluorescence spectra of L2 (10 μM) in DMSO: H₂O (3:2, v/v, 10 mM HEPES buffer, pH = 7) in the presence of 3 equivalents of various metal ions. $\lambda_{\text{ex}} = 360$ nm; slit = 10 /10 nm

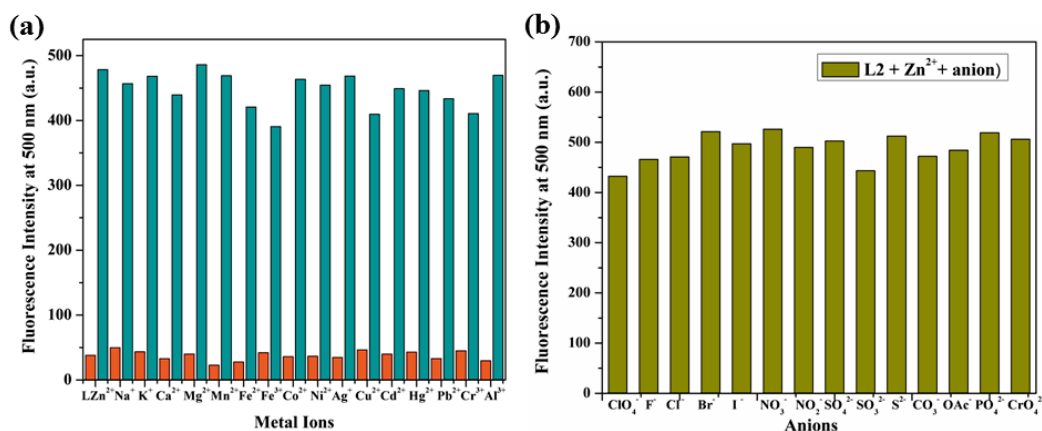


Fig. 2. (a) Selectivity of the dye L2 (10 μM) for the Zn^{2+} in DMSO: H₂O (3:2, v/v, 10 mM HEPES buffer, pH = 7) in the presence of 10 equivalents of various metal ions. Red bars indicate the emission responses of the dye with 10 equiv. of the metal ions of interest, and blue bars represent the final integrated fluorescence response after the addition of 3 equivalents of Zn^{2+} to each solution containing other metal ions (b) Selectivity of the dye L2 (10 μM) for the Zn^{2+} in DMSO: H₂O (3:2, v/v, 10 mM HEPES buffer, pH = 7) in presence 10 equivalents of different anions. $\lambda_{\text{ex}} = 360$ nm; slit = 10/10 nm

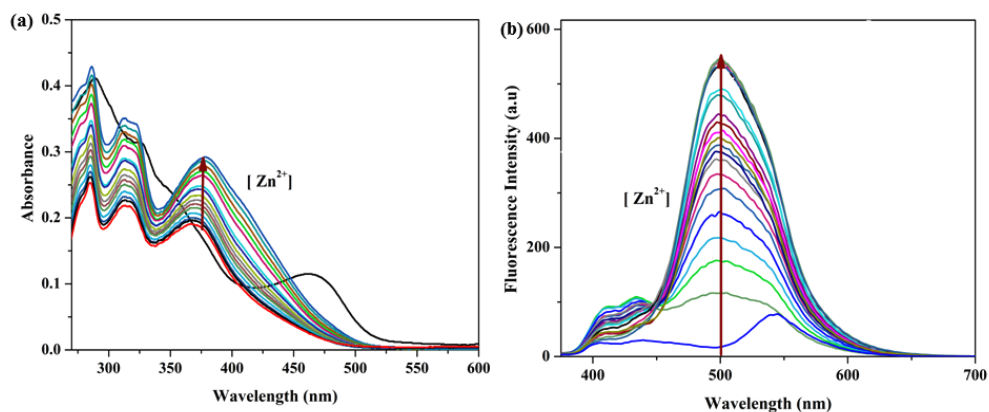


Fig.3. (a) Absorption titration (b) fluorescence titration of L2 with increasing Zn²⁺ ions concentration in DMSO: H₂O (3:2, v/v, 10 mM HEPES buffer, pH = 7) Arrow indicates the increasing trend in Zn²⁺ ion concentration (0-20 μM). λ_{ex} = 360 nm ; slit = 10 /10 nm

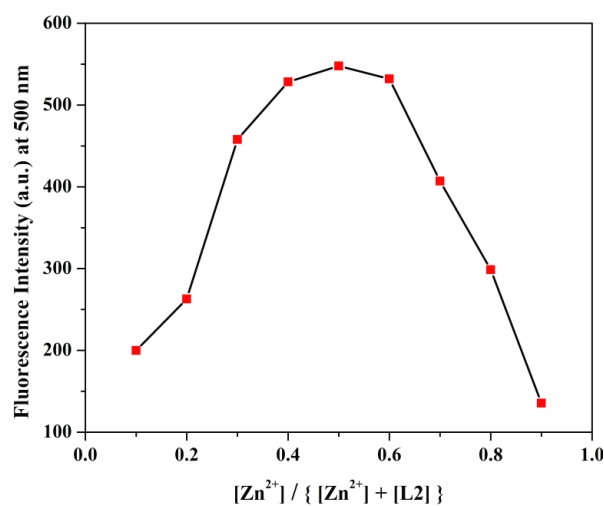


Fig. 4. Job's plot for determination of binding stoichiometry between L2 and Zn²⁺

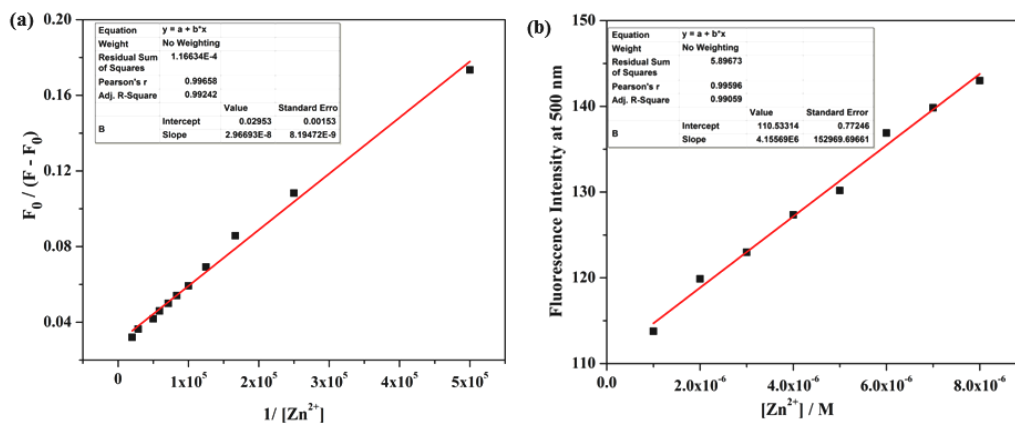


Fig.5. (a) Binding constant plot of L2 for Zn²⁺ (b) Linear response curve of L2 at 500 nm depending on the Zn²⁺ ion concentration for determination of lowest detection limit
3.2. ¹H NMR titration

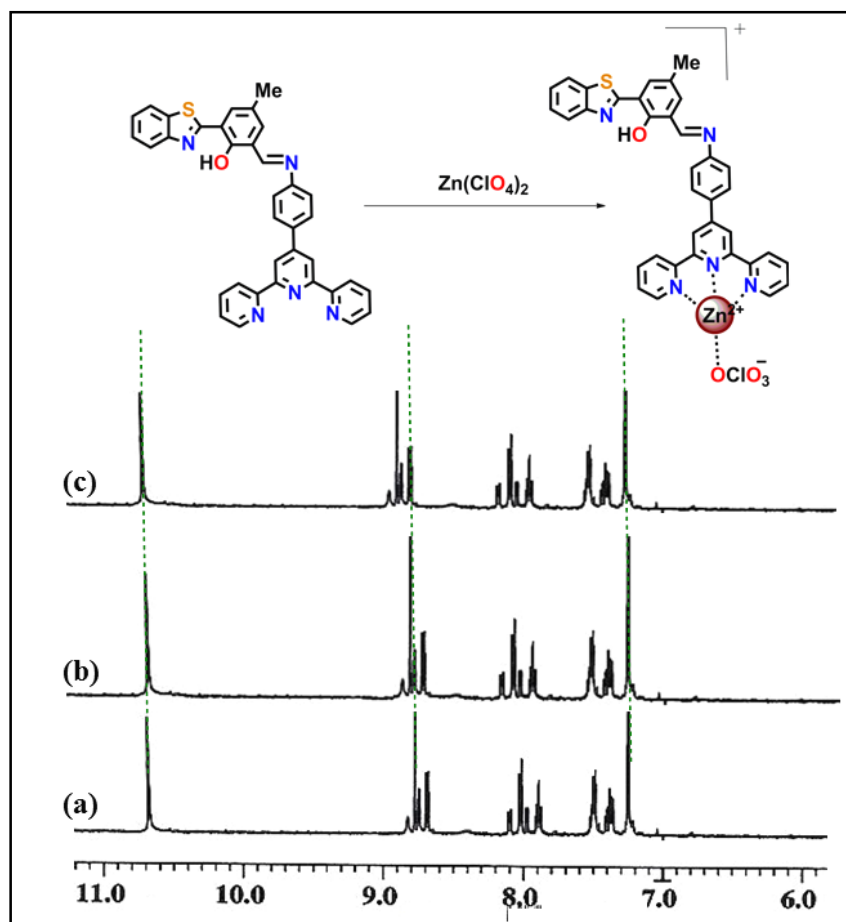


Fig. 6. Proposed binding mode of L2 with Zn^{2+} . (a) L2 only, (b) L2 and 0.5 equivalent of Zn^{2+} , (c) L2 and 1 equivalent of Zn^{2+}

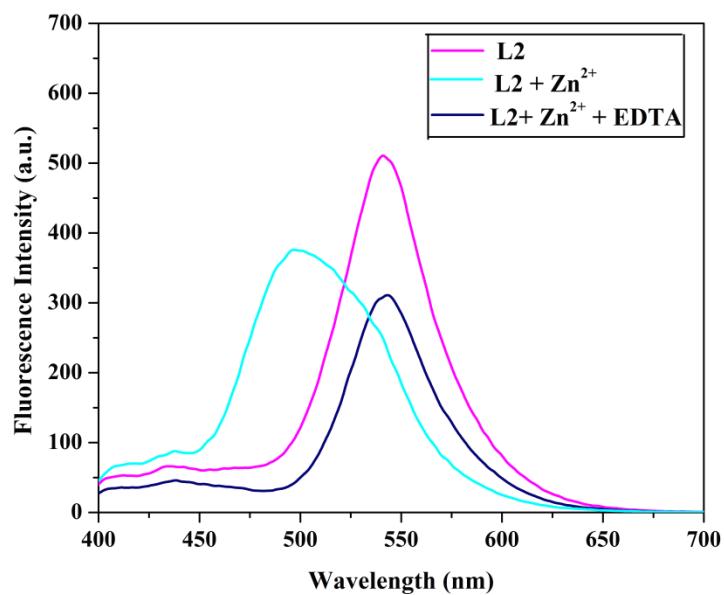


Fig. 7. Reversible nature of L2 in Zn^{2+} sensing process in presence of excess of EDTA

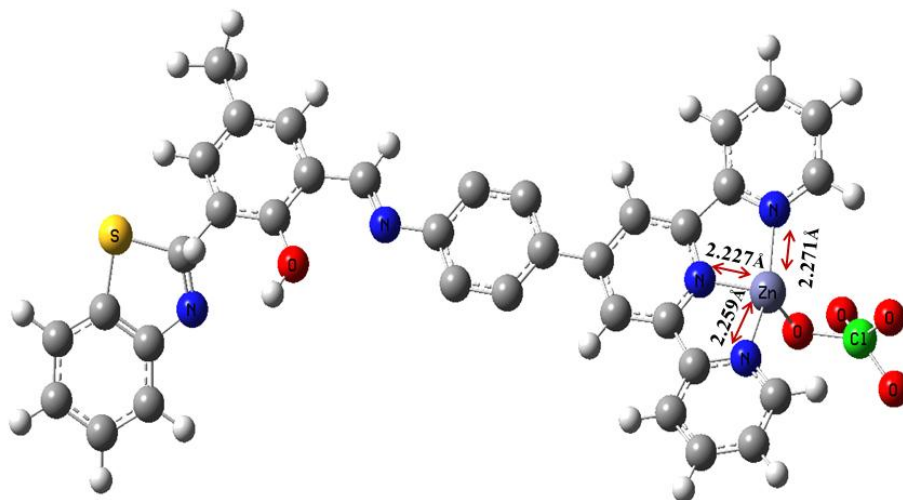


Fig.8 DFT Optimized structure of L2- Zn^{2+} complex

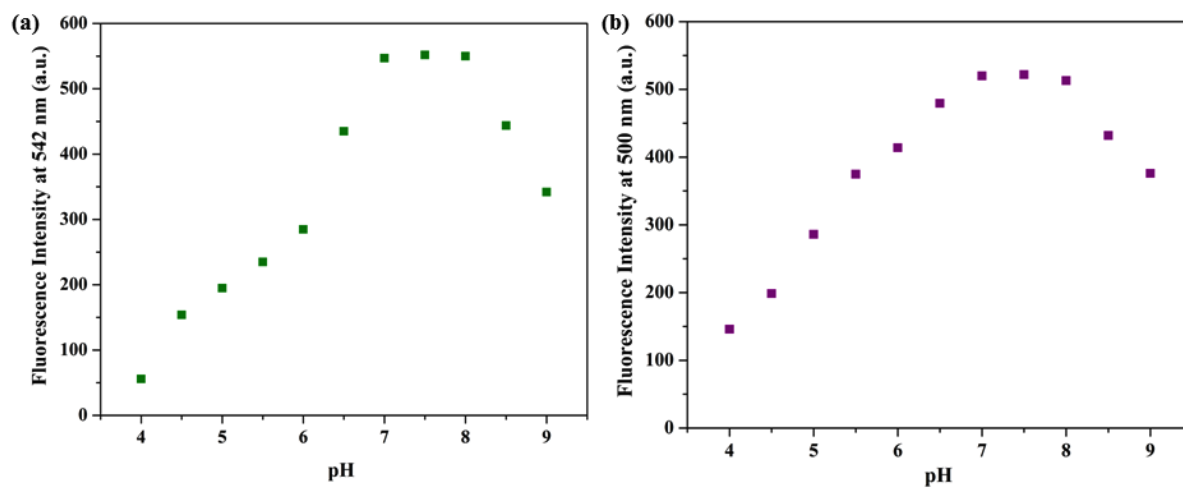
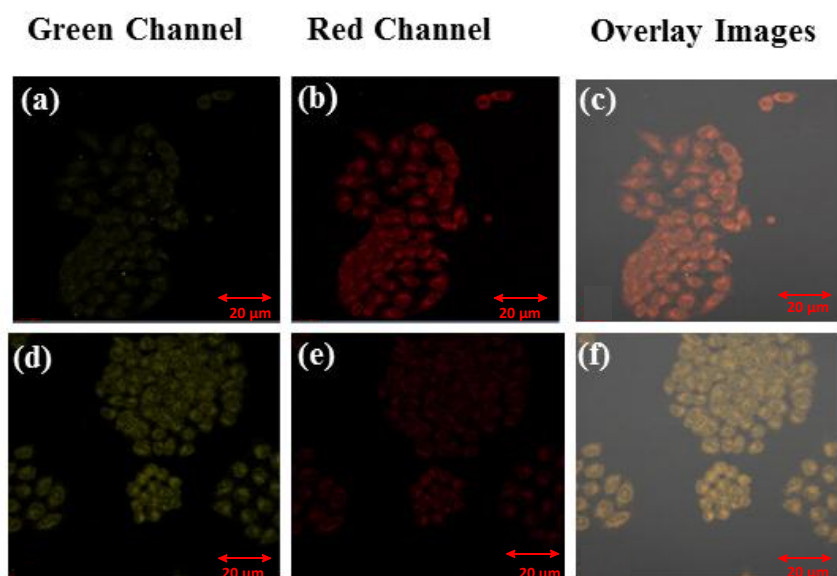


Fig. 9. The fluorescence intensity changes (a) of L2 at 542 nm and (b) of L2-Zn²⁺ solution at 500 nm under various pH conditions. $\lambda_{\text{ex}} = 360 \text{ nm}$; slit = 10 /10 nm.



<InlineShape2>

Fig.10. Biosensing of Zn^{2+} in HeLa cells. Fluorescence images of HeLa cells first incubated with L2 ($10\ \mu M$) for 30 min and then zinc perchlorate ($10\ \mu M$) for 1 h, (a) fluorescence image of L2 in green channel (b) fluorescence image of L2 in red channel (c) The overlay images of (a) & (b), (d) fluorescence image of L2 after incubated with zinc perchlorate in green channel (e) fluorescence image of L2 after incubated with zinc perchlorate in red channel (f) The overlay images of (d) & (e). Scale bar is $20\ \mu m$

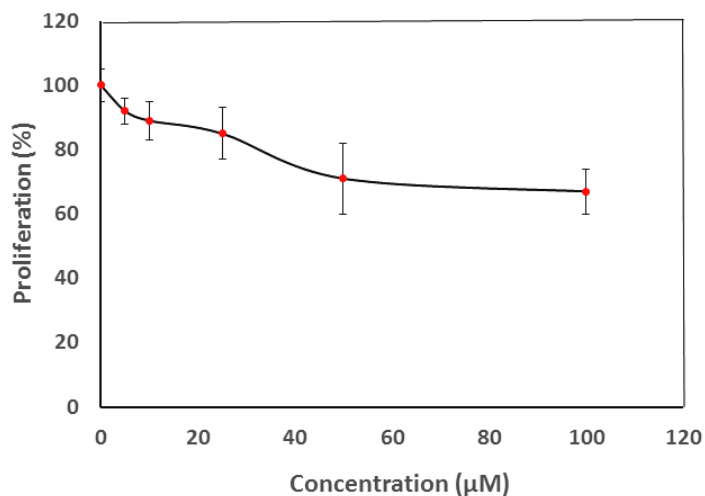


Fig.11. Cellular cytotoxicity assessment of different concentrations of sensor L2 in HeLa cell lines